Observation of three-quasiparticle structures in the $N=88$ nucleus ^{153}Tb

D. J. Hartley, T. B. Brown, F. G. Kondev, R. W. Laird, J. Pfohl, A. M. Richmond, and M. A. Riley
Department of Physics, Florida State University, Tallahassee, Florida 32306

J. Döring
Department of Physics, University of Notre Dame, Notre Dame, Indiana 46556

J. Simpson
CCLRC, Daresbury Laboratory, Daresbury, Warrington, WA4 4AD, United Kingdom

(Received 14 April 1998)

High-spin states of ^{153}Tb were populated via the reaction ^{139}La(^{18}O,4n) at a beam energy of 100 MeV. Previously known bands have been extended beyond the region of the first $i_{13/2}$ neutron alignment and two new structures have been identified. The rotational alignment behavior of the $\pi h_{11/2}$ and new bands are discussed. Quasiparticle assignments are suggested for the latter. $B(M1)/B(E2)$ ratios were extracted and compared to theoretical calculations. [S0556-2813(98)05508-3]

PACS number(s): 21.10.Re, 23.20.Lv, 27.70.+q

A stark contrast is observed between the largely single-particle structure in $N=82$–86 nuclei and the collective rotational structure of the $N\geqslant 90$ nuclei. The $N=88$ nuclei act as the bridge between these two classes of nuclear behavior. In addition, the transitional $N=88$ nuclei near Gd are the heaviest nuclei still under the influence of the $Z=64$ subshell gap. Although these nuclei have enough valence particles to sustain rotational structures, they are significantly less deformed than the $N\geqslant 90$ nuclei where the subshell gap is apparently eliminated [1]. These features partially fueled the interest in the present study of $^{153}_{65}$Tb$_{88}$, which is a part of our systematic investigation of the $N=88$, 90 [2,3], and 92 [4] terbium nuclei. We are particularly interested in the $\pi h_{11/2}$ bands of these nuclei such that a comprehensive study of the signature splitting in the odd-$A\approx 160$, $\pi h_{11/2}$ bands could be performed [2,3]. Therefore, in this work, we will concentrate on this negative-parity band and the two new three-quasiparticle structures in ^{153}Tb.

High-spin states of ^{153}Tb were populated using the reaction ^{139}La(^{18}O,4n) at a beam energy of 100 MeV. The beam was provided by the Florida State University tandem-linac accelerator facility and the de-exciting γ rays were detected with the Florida State University array [5]. Five high-purity Ge detectors, surrounded with bismuth germanate (BGO) shields for Compton suppression, were used in the array with two located at 145° and three at 90° with respect to the beam direction. A single, self-supporting foil of natural La with a thickness of ≈ 70 mg/cm^2 was used for this experiment. Over 140 million events were recorded when at least two detectors fired within a prompt coincidence window (100 ns). The data were sorted into an $E_\gamma \times E_\gamma$ symmetric matrix which was inspected with the program ESCL8R [6]. Energy calibrations and detector efficiencies were determined with an ^{152}Eu source. Directional correlation of oriented states (DCO) data sorting and analysis were performed in order to determine the spins of new energy levels.

The level scheme of ^{153}Tb is displayed in Fig. 1. The $\pi h_{11/2}$ and [404]7/2 bands were significantly extended from the previous spin values [7,8] of $I^\pi=\frac{35}{2}^-$ and $\frac{27}{2}^+$ to ($\frac{57}{2}^-$) and ($\frac{41}{2}^+$), respectively. The band built upon the [402]5/2 ground state [9] was confirmed, but could not be extended. Two high-spin sequences were observed for the first time and are labeled as bands 1 and 2. The spins of the states that could not be determined by DCO analysis, due to the weak intensity of the depopulating transition, are placed within parentheses in the level scheme. Tentative transitions and states are denoted by dashed lines in Fig. 1.

The band based on a mixture of the low-K orbitals from the $h_{11/2}$ proton shell is built on the isomeric ($T_{1/2}=173$ μs [10]) $I^\pi=\frac{11}{2}^-$ state at 163.3 keV. This isomer feeds the $\frac{7}{2}^+$state of the [404]7/2 band by an 82.6 keV $M2$ transition [10], which was not observed in our data due to the relatively long lifetime of the $\frac{11}{2}^-$ state and the high electron conversion coefficient ($\alpha_T\approx 150$ [11]). A coincidence spectrum of the $\pi h_{11/2}$ band is shown in Fig. 2(a). The high-energy insert of Fig. 2(a) is a coincidence spectrum from the 733.7 keV γ ray ($\frac{49}{2}^- \rightarrow \frac{45}{2}^-$), which displays transitions depopulating some of the highest spin states in the band. The $\alpha=-\frac{1}{2}$ signature is favored over its partner below spin $I=\frac{33}{2}$; however, above this spin value, neither signature is significantly favored over the other (see Fig. 1). This quenching of the signature splitting has been observed in the nearby $N\geqslant 90$ odd-Z nuclei, but it is not as dramatic as in the $N=88$ ^{151}Eu [12,13], ^{153}Tb, ^{155}Ho [14], ^{157}Tm [15], and ^{159}Lu [16] nuclei. The alignment of the $i_{13/2}$ neutrons is suspected [17–19] to be responsible for this loss of signature splitting as they drive the nucleus from triaxial (nonsymmetric) to more prolate symmetric shapes. A full systematic study of the experimental signature splitting in the $\pi h_{11/2}$ bands of the odd-Z, odd-$A\approx 160$ region will be given in Ref. [3].

Band 1 feeds the [404]7/2 band directly through the 485.0 [$R_{\rm DCO}=1.1(1)$] and 688.0 keV [$R_{\rm DCO}=1.1(1)$] $\Delta I=2$ transitions, thus suggesting a positive-parity assignment to the band and a spin of $\frac{27}{2}^+$ to the lowest observed state. Band 1 also decays directly into the $\pi h_{11/2}$ band through the 211.7 [$R_{\rm DCO}=0.7(1)$] and 516.4 keV [$R_{\rm DCO}=0.6(1)$] dipole tran-

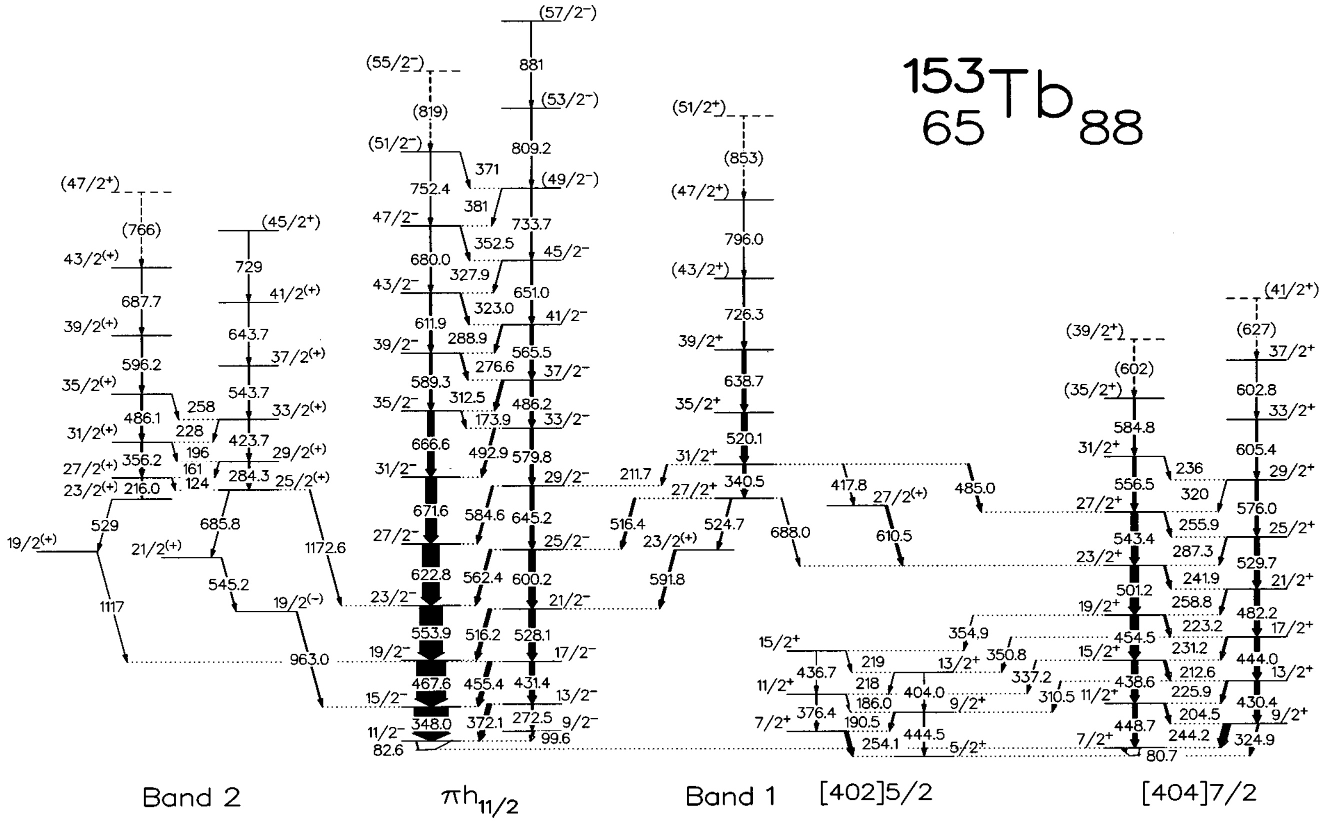

FIG. 1. The level scheme of ^{153}Tb. The widths of the arrows are proportional to the relative intensity of the transitions.

sitions, which are consistent with the band feeding an opposite-parity structure. The lack of an observed signature partner indicates that band 1 most likely has a low-K value.

The decay of band 2 to the $\pi h_{11/2}$ band is fragmented between intermediate states and one direct high-energy linking transition. Analysis of the intensity of band 2 indicates that more decays out of the band must also be present, but were not identified. The 1172.6 keV linking γ ray has a $R_{\mathrm{DCO}}=0.5(1)$, which suggests that it has dipole character; therefore, the state at 2705.4 keV is assigned a spin of $\frac{25}{2}$. A spectrum of the transitions in coincidence with the 1172.6 keV γ ray is shown in Fig. 2(b). Band 2 has essentially no signature splitting and thus it likely arises from a high-K configuration. This assignment is consistent with the observed fragmented decay path to the $\pi h_{11/2}$ band through states that possibly have intermediate K values.

The alignments of the $\pi h_{11/2}$ band, band 1, and band 2 in ^{153}Tb are plotted in Fig. 3. The Harris parameters $\mathcal{J}_0=12$ $\hbar^2$/MeV and $\mathcal{J}_1=90$ $\hbar^4$/MeV^3 are chosen such that the ground-state band in the even-even core nucleus ^{152}Gd [20] has nearly zero initial alignment.

The high alignment ($i\approx 4$ $\hbar$) of the $\pi h_{11/2}$ band at low rotational frequency ($\hbar\omega<0.25$ MeV) is characteristic of a band based on a high-j, low-K orbital. The large gain in alignment, observed in both signatures with $\Delta i=10.8$ $\hbar$, is attributed to the lowest pair of $i_{13/2}$ neutrons aligning their spins along the nuclear rotation axis (which is known as the AB crossing [21]). This crossing occurs at a rotational frequency of 0.284(3) and 0.318(3) MeV for the $\alpha=+\frac{1}{2}$ and $\alpha=-\frac{1}{2}$ signatures, respectively. The difference is a result of the $\alpha=-\frac{1}{2}$ signature being energetically favored below the crossing region and the fact that at high rotational frequency neither signature is strongly favored. The systematics of the AB crossing in the $\pi h_{11/2}$ bands for odd-Z nuclei near terbium has been discussed in Ref. [4].

Band 1 has a nearly constant alignment at $i\approx 12.5$ $\hbar$ and passes through the AB band crossing region (see Fig. 3). Since the AB crossing is blocked, an $i_{13/2}$ neutron is likely to be involved in the quasiparticle configuration. Although band 1 shows evidence for the beginning of a crossing (most likely the BC) at the highest observed frequencies, no definitive crossings can be identified in this band. However, a similar band has been observed in ^{155}Tb [3] and experiences both the BC and B_pC_p crossings. This suggests that the A $(\pi,\alpha)=(+,+\frac{1}{2})$ $i_{13/2}$ neutron and A_p $(-,-\frac{1}{2})$ $h_{11/2}$ proton are involved in the initial configuration. These quasiparticles are also likely to be associated with band 1 in ^{153}Tb. Therefore, the third quasiparticle would likely come from a negative-parity neutron orbital near the Fermi surface and have $\alpha=-\frac{1}{2}$ in order to give the band the experimentally determined positive-parity and $\alpha=-\frac{1}{2}$ signature, respectively. Either the favored signature of the $f_{7/2}$ neutron orbital or the unfavored signature of the $h_{9/2}$ orbital are possible choices, although it should be noted that these orbitals are strongly mixed with each other. Since the $\alpha=+\frac{1}{2}$ signature of the $h_{9/2}$ bands in the $N=89$ nuclei ^{153}Gd [22] and ^{155}Dy [22,23] have been observed to be favored over the $\alpha=-\frac{1}{2}$ signature, we suggest that band 1 has as its major component the $\pi h_{11/2}\otimes\nu(i_{13/2}f_{7/2})$ configuration. In cranked shell model nomenclature [21], this band would be labeled as $A_p\otimes AF$. However, the $B_p\otimes AE$ configuration cannot be completely ruled out since the band crossings observed in the ^{155}Tb band, particularly the B_pC_p, have not been identified in band 1 of ^{153}Tb. Either configuration would be consistent with the

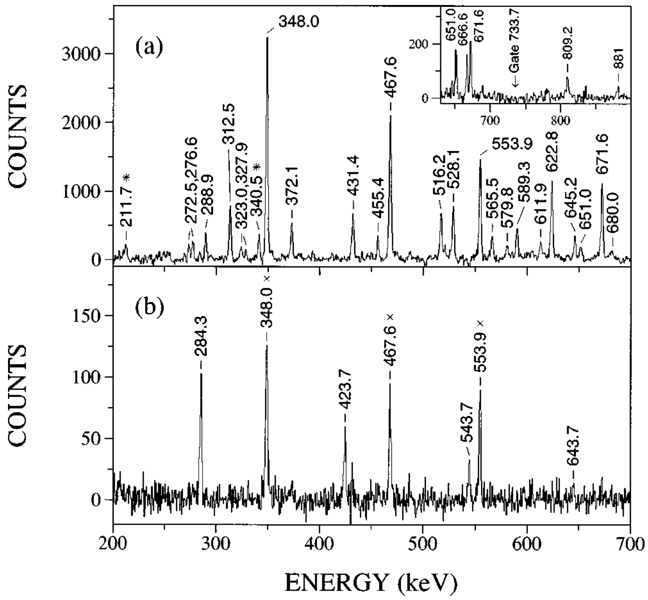

FIG. 2. (a) Spectrum of transitions in coincidence with the 600.2 and 666.6 keV γ rays in the $\pi h_{11/2}$ band. The transitions marked with asterisks are γ rays from band 1. The high-energy insert contains a spectrum of transitions in coincidence with the 733.7 keV γ ray. (b) Coincidence spectrum of band 2 which results from γ rays in coincidence with the 1172.6 keV linking transition. Peaks marked with crosses in panel (b) are the three strongest transitions in the $\pi h_{11/2}$ band.

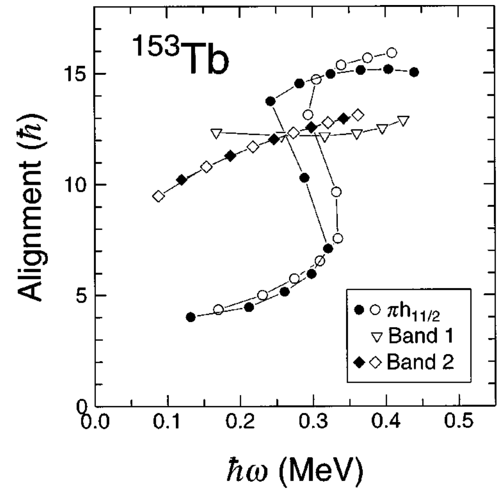

FIG. 3. The alignment of the $\pi h_{11/2}$ band, band 1, and band 2 in ^{153}Tb plotted versus rotational frequency $\hbar\omega$. The K values $\frac{3}{2}$, $\frac{5}{2}$, and $\frac{15}{2}$ were used for the $\pi h_{11/2}$ band, band 1, and band 2, respectively. The solid and open symbols represent the $\alpha=+\frac{1}{2}$ and $\alpha=-\frac{1}{2}$ signatures, respectively.

experimentally observed $\approx 8\ \hbar$ difference in alignment between band 1 and the $\pi h_{11/2}$ band at low rotational frequency ($\hbar\omega<0.25$ MeV). The $A_p\otimes AF$ or $B_p\otimes AE$ assignment agrees well with the depopulation of band 1 into the $\pi h_{11/2}$ band as a result of the neutrons re-coupling and the decays into the [404]7/2 band are a product of the close lying interacting positive-parity states.

The large initial alignment (see Fig. 3) and excitation energy of band 2 also indicate that it has a three-quasiparticle structure. Similar to band 1, band 2 does not undergo the AB crossing implying that at least one $i_{13/2}$ neutron is involved in the configuration. The decay into the $\pi h_{11/2}$ band also suggests that an $h_{11/2}$ quasiproton is associated with this band. Both of these quasiparticles are low K; therefore, in order to give band 2 a high-K configuration, as its experimental properties suggest, a high-K quasineutron must be included as the third quasiparticle. The only high-K neutron orbital near the Fermi surface of ^{153}Tb is the $\nu h_{11/2}$ [505]11/2 orbital, and so we suggest that band 2 has the $\pi h_{11/2}\otimes\nu(i_{13/2}h_{11/2})$ configuration with the signature partners resulting from the two equally favored signatures of the $h_{11/2}$ neutron. Following the quasiparticle labeling convention of Ref. [24], this would be the $A_p\otimes AX(Y)$ band [although again the $B_p\otimes AX(Y)$ cannot be ruled out]. This configuration was also given to a similar band in ^{157}Ho (band 6 in Ref. [25]) and the *AX(Y)* two-quasineutron excitation has been identified in the neighboring even-even ^{154}Dy [26] nucleus. The difference of 6.4 $\hbar$ in alignment between band 2 and the $\pi h_{11/2}$ band is consistent with either configuration.

The $B(M1)/B(E2)$ transition strength ratios [27] were extracted from the $\pi h_{11/2}$ band and band 2 in ^{153}Tb. Theoretical calculations of the $B(M1)/B(E2)$ ratios were also performed using an extended formalism [28] of the geometrical model from Dönau [29] and Frauendorf [30]. The parameters used in the calculations are summarized in Table I. The intrinsic quadrupole moment Q_0 of the $\pi h_{11/2}$ band was estimated by averaging the measured quadrupole moments of the neighboring even-even nuclei [31]. The gyromagnetic ratio of the collective motion was taken as $g_R=0.7Z/A$ and the g_K values for the protons were determined by a Woods-Saxon calculation [32]. The alignments for the quasiparticles were extracted from Fig. 3, and the results of the $B(M1)/B(E2)$ analysis are shown in Fig. 4.

The $B(M1)/B(E2)$ ratios of the $\pi h_{11/2}$ band are quite low at $\approx 0.1\ (\mu_N/e\ \mathrm{b})^2$ in the low-spin region ($I<\frac{33}{2}$) which is reproduced by the theoretical calculations (see Fig. 4), but above spin $\frac{33}{2}$, the $B(M1)/B(E2)$ ratios increase significantly. This increase is associated with the alignment of a pair of $i_{13/2}$ neutrons and has been reproduced by the theoretical calculations (solid line above $I=\frac{33}{2}$). While the theory is in reasonable agreement with the $\alpha=+\frac{1}{2}$ signature, the experimental $B(M1)/B(E2)$ ratios for the $\alpha=-\frac{1}{2}$ signature are somewhat higher. The strong signature dependence of the $B(M1)/B(E2)$ ratios after the *AB* crossing occurs in a spin region where the splitting in the energy levels is nearly quenched (see Fig. 1). Other $N=88$ nuclei, e.g.,

TABLE I. Parameters used in the calculation of $B(M1)/B(E2)$ ratios for the bands in ^{153}Tb.

Band	$Q_0(e\ \mathrm{b})$	g_R	$g_K(\pi)$	$K(\pi)(\hbar)$	$i(\pi)(\hbar)$	$g_K(\nu)$	$K(\nu)(\hbar)$	$i(\nu)(\hbar)$
$\pi h_{11/2}$	4.6	0.30	1.51	3/2	4.0	−0.20	0	10.8
Band 2	4.6	0.30	1.41	5/2	4.0	−0.50	5	6.4

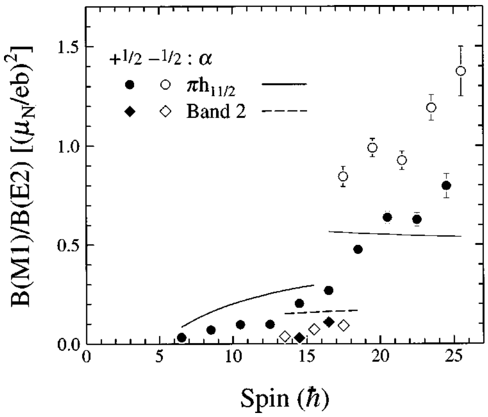

FIG. 4. The experimental and theoretical $B(M1)/B(E2)$ ratios for the $\pi h_{11/2}$ band and band 2 in ^{153}Tb. The solid and open symbols represent the $\alpha=+\frac{1}{2}$ and $\alpha=-\frac{1}{2}$ signatures, respectively.

^{151}Eu, ^{155}Ho, and ^{157}Tm, also exhibit similar behavior.

The low $B(M1)/B(E2)$ ratios in band 2 (see Fig. 4) are very similar to those observed in the $A_p \otimes AX(Y)$ band of ^{157}Ho [25]. The g_K value for the neutrons in band 2 was determined by fitting the *AX(Y)* band in ^{154}Dy [26]. The calculations for ^{153}Tb are extremely sensitive to the K value of the $h_{11/2}$ proton orbital. Using $K=\frac{3}{2}$, $B(M1)/B(E2)$ ratios of over 0.8 $(\mu_N/e\ b)^2$ were calculated. It is only when the $K=\frac{5}{2}$ value is used that a reasonable agreement with the experimental data is obtained. This is consistent with the suggestion [33] that the *AX(Y)* configuration drives towards larger deformation and thus moves the proton Fermi surface closer to the [532]5/2 orbital in ^{153}Tb. The increased deformation, which is not included in the calculations shown in Fig. 4, would also be consistent with the slight overestimation in the calculated ratios compared to the experimental data.

In summary, rotational structures in the weakly deformed ^{153}Tb nucleus were observed for the first time with rotational frequencies at and beyond the first $i_{13/2}$ neutron alignment. Over 70 new transitions have been placed in the level scheme and two new three-quasiparticle structures have been observed. Configuration assignments have been made for the new bands from the analysis of their respective alignment behavior and comparisons of experimental and theoretical $B(M1)/B(E2)$ values.

Special thanks to D.C. Radford and H.Q. Jin for their software support. Support for this work was provided by the National Science Foundation, the State of Florida, and the U.K. Engineering and Physical Science Research Council. M.A.R. and J.S. acknowledge the receipt of a NATO Collaborative Research Grant. A.M.R. acknowledges the support of NSF REU, Contract No. 1334 601 22.

[1] R.F. Casten, D.D. Warner, D.S. Brenner, and R.L. Gill, Phys. Rev. Lett. **47**, 1433 (1981).
[2] M.A. Riley *et al.*, Phys. Rev. C **53**, 989 (1995).
[3] D.J. Hartley *et al.*, Phys. Rev. C (submitted).
[4] D.J. Hartley *et al.*, Phys. Rev. C **57**, 2944 (1998).
[5] S.L. Tabor *et al.*, Nucl. Instrum. Methods Phys. Res. B **79**, 821 (1993).
[6] D.C. Radford, Nucl. Instrum. Methods Phys. Res. A **361**, 297 (1995).
[7] G. Winter, J. Döring, L. Funke, P. Kemnitz, E. Will, S. Elfström, S.A. Hjorth, A. Johnson, and Th. Lindblad, Nucl. Phys. **A299**, 285 (1978).
[8] M.D. Devous, Sr. and T.T. Sugihara, Z. Phys. A **288**, 79 (1978).
[9] B. Harmatz and T.H. Handley, Nucl. Phys. **A191**, 497 (1972).
[10] M.D. Devous, Sr. and T.T. Sugihara, Phys. Rev. C **15**, 740 (1977).
[11] F. Rösel, H.M. Fries, K. Alder, and H.C. Pauli, At. Data Nucl. Data Tables **21**, 291 (1978).
[12] W.J. Vermeer, W. Urban, M.K. Khan, C.J. Pearson, A.B. Wiseman, B.J. Varley, J.L. Durell, and W.R. Phillips, Nucl. Phys. **A559**, 422 (1993).
[13] J.R. Jongman, W. Urban, J.C.S. Bacelar, J. van Pol, J. Nyberg, G. Sletten, J.S. Dionisio, Ch. Vieu, J.M. Lagrange, and M. Pautrat, Nucl. Phys. **A591**, 244 (1995).
[14] J. Simpson *et al.* (unpublished).
[15] M.A. Riley *et al.*, Phys. Rev. C **51**, 1234 (1995).
[16] Y. Ma, H. Sun, Y. Liu, S. Wen, H. Zheng, S. Li, G. Li, G. Yuan, P. Weng, and C. Yang, J. Phys. G **21**, 937 (1995).
[17] S. Frauendorf and F.R. May, Phys. Lett. **125B**, 245 (1983).
[18] Y.S. Chen, S. Frauendorf, and L.L. Riedinger, Phys. Lett. B **171**, 7 (1986).
[19] I. Hamamoto and H. Sagawa, Phys. Lett. B **201**, 415 (1988).
[20] D.R. Zolnowski, M.B. Hughes, J. Hunt, and T.T. Sugihara, Phys. Rev. C **21**, 2556 (1980).
[21] R. Bengtsson, S. Frauendorf, and F.-R. May, At. Data Nucl. Data Tables **35**, 15 (1986).
[22] T.B. Brown *et al.* (unpublished).
[23] R. Vlastou *et al.*, Nucl. Phys. **A580**, 133 (1994).
[24] M.A. Riley *et al.*, Nucl. Phys. **A486**, 456 (1988).
[25] D.C. Radford *et al.*, Nucl. Phys. **A545**, 665 (1992).
[26] W. C. Ma (private communication).
[27] A. Bohr and B.R. Mottelson, *Nuclear Structure* (Benjamin, New York, 1975), Vol. 2.
[28] V.P. Janzen *et al.*, Phys. Rev. C **45**, 613 (1992).
[29] F. Dönau, Nucl. Phys. **A471**, 469 (1987).
[30] S. Frauendorf, Phys. Lett. **100B**, 219 (1981).
[31] S. Raman, C.H. Malarkey, W.T. Milner, C.W. Nestor, Jr., and P.H. Stelson, At. Data Nucl. Data Tables **36**, 1 (1987).
[32] S. Ćwiok, J. Dudek, W. Nazarewicz, J. Skalski, and T. Werner, Comput. Phys. Commun. **46**, 379 (1987); J. Dudek, A. Majhofer, J. Skalski, T. Werner, S. Ćwiok, and W. Nazarewicz, J. Phys. G **5**, 1359 (1979).
[33] J.D. Morrison, J. Simpson, M.A. Riley, H.W. Cranmer-Gordon, P.D. Forsyth, D. Howe, and J.F. Sharpey-Schafer, J. Phys. G **15**, 1871 (1989).